

PASSIVE L-BAND RADIOMETER FOR REMOTE SENSING OF EARTH RESOURCES

By

T. Flattau, S. Becker, and A. Leber

AIL, a division of Cutler-Hammer
Melville, New York 11746

Abstract

The features of an orbiting L-band microwave radiometer experiment carried onboard the NASA Skylab satellite are described. Some typical data and their usefulness are also presented so that both the instrument and its utility may be appreciated.

Introduction

The remote measurement of the earth's upwelling thermal emission with a passive microwave radiometer permits the monitoring of selected earth resources.^{1, 2} This paper describes an L-band radiometer (Experiment S-194) which was mounted on the NASA Skylab spacecraft and used to remotely determine the soil moisture content over various types of terrain. In addition, the salinity content of water was used to correlate measured S-194 radiometer data over selected maritime locations.

Unique features of the TRF type radiometer front-end include a 15-pole band-pass filter, a 5-pole PIN diode microwave switch, and precision temperature-controlled hot and cold reference noise generators for use in an unattended calibration sequence. In addition, a new type of radiometer processing technique and a 64-element linear array antenna were developed. Measured and calculated L-band earth brightness temperatures for a typical satellite ground track pass will also be presented.

Mission Profile

The spacecraft was launched in May 1973; the NASA manned mission extended through February 1974. The Skylab orbit included a mean altitude and inclination of 439 km (237 nmi) and 50 degrees, respectively. In addition, a 5-day repeating orbital period of 93 minutes each was achieved at an altitude velocity of 7.65 km/second.

The 21.4-cm wavelength (1.41 GHz) L-band radiometer was mounted on the spacecraft's exterior surface to provide a nadir ground footprint of 115 km (62 nmi). Scientific data was digitally recorded on magnetic tape and subsequently returned to earth by the onboard manned crew. Data processing was performed at NASA/JSC, and the analysis and interpretation data by the scientific community are still continuing.^{3, 4, 5}

Radiometric Design Concepts

The L-band radiometer frequency range was selected to coincide with the 1.400 to 1.427 GHz radio astronomy band in order to effectively eliminate interference effects due to RF emitters. In addition, this frequency range exhibits minimal atmospheric absorp-

tion effects, and thereby offers all-weather radiometric operation. Furthermore, radiometric measurements in this frequency region include subsurface emission effects, which can be related to either the soil moisture of selected land areas, or the salinity concentration of maritime regions.⁶

A TRF radiometer front-end was chosen as the simplest configuration to effectively eliminate possible noise and spurious response problems normally associated with the mixer and local oscillator combination used with superheterodyne receiver front-ends.

A self-calibrating, Dicke-switched radiometer was developed for reliable unattended operation in deep space. Possible radiometric measurement errors were reduced by minimizing reflection interaction effects between the antenna and the Dicke-switch, and associated connecting loads. In addition, the absolute temperatures of the reference and calibration terminations were carefully controlled and continuously monitored.

The possibility of measurement errors due to radiometer variations in a space environment was considered; a new signal processing technique was developed to minimize such risks. A self-balancing technique was incorporated to vary the system video gain in synchronism with the radiometric temperatures associated with each position of the Dicke-switch. With this technique, a measurement of temperature ratio is obtained; errors due to gain variation are effectively eliminated.

A planar array antenna was developed to provide a low-loss and high efficiency transducer with controlled beam width characteristics. These characteristics are considered essential since they are the determining factors with respect to antenna performance in a radiometric application.

Radiometer Receiver and Antenna

A simplified block diagram of the Dicke-switched L-band radiometer is shown in Fig. 1.

The low-loss SP5T L-band switch⁷ employed 15 PIN diodes in a series-shunt configuration, and exhibited a VSWR of 1.02 and an isolation of 35 dB. The RF switch operated at a 105-Hz switching rate; four of the switch arms were connected to radiometric hot (370 K) and cold (200 K) load noise generators. The

cold load generators are shown in Fig. 2. The precision radiometric reference terminations⁸ were temperature controlled to within 0.1 K, and provided VSWR's less than 1.10.

The TRF receiver front-end included a 9-section, 4-GHz, low-pass filter, and a 4-section (54-MHz bandwidth) and a 15-section (27-MHz bandwidth) band-pass filter to provide controlled frequency selectivity. In addition, transistor RF pre- and post-amplifiers were used to provide an overall gain of 77 dB in order to ensure optimum square law detection over a radiometric temperature range of 0 to 400 K.

The radiometer back-end contained a unique self-balancing gain modulation processor⁹ to eliminate the effects of gain variation and also to provide rapid transient response.

A 64-element L-band planar array antenna with 93-percent efficiency, and a 3-dB beam width of 15 degrees and a first null beam width of less than 40 degrees is used to collect the upwelling thermal radiation. The antenna was constructed using microstrip techniques and provides a single coaxial output. The antenna weight was 33 pounds, and corresponding radiometer receiver weight was 20 pounds.

Performance

The L-band radiometer exhibited temperature sensitivities of less than 0.5 K, and accuracies of better than 0.7 K at a source temperature of 296 K for an RF bandwidth of 27 MHz and an integration time of 1 second. In addition, long-term drift was measured to be less than 0.2 K.

An example of a satellite ground track over Baja, California, and the resultant earth brightness temperatures⁶ are shown in Figs. 3 and 4. As can be seen, the predicted and measured L-band earth brightness temperatures were in excellent agreement.

Soil Moisture

Soil moisture determination is of great importance to certain specialized segments of the scientific community. The meteorologist is interested in soil moisture since it is a factor in the atmospheric heat exchange balance over land areas. Similarly, the hydrologist is interested in soil moisture since it affects the surface water runoff and flooding conditions over selected ground boundaries. The agriculturalist is also keenly interested in soil moisture since it greatly affects vegetation growth, plant disease, and the forecast of crop yield.

Remote sensing of soil moisture with the Skylab L-band radiometer data has been examined; excellent correlation has been obtained with ground truth information.^{3,4}

It has been determined that the surface 2.5-cm soil moisture depth is the major contributing emission layer, although radiometric data correlation was obtained at surface depths down to 15 cm. In addition, the data analysis has disclosed that L-band radiometry is extremely sensitive to soil moisture

changes, with 1-percent soil moisture increase resulting in 2.5 K decrease in corresponding radiometric data (over a measured soil moisture range of 0 to 35 percent by weight).

It should be noted that other radiometric soil moisture investigations are continuing;^{10, 11, 12} it is expected that additional soil moisture remote sensing radiometers will be launched in future satellite programs.

References

1. K. Tomiyasu, "Remote Sensing of the Earth by Microwaves," Proc of the IEEE, 62, p 86-88, January 1974.
2. D. Staelin, "Passive Microwave Sensing of the Earth," IEEE GMTT International Symposium, 1975.
3. J. Eagleman, "Moisture Detection From Skylab," Proc of Ninth International Symposium on Remote Sensing of Environment, Vol I, p 701-705, 19 April 1974.
4. M. McFarland, "The Correlation of Skylab L-Band Brightness Temperatures with Antecedent Precipitation," University of Oklahoma WEAT Report No. 17, February 1975.
5. F. Ulaby, L. Dellwig, and T. Schmugge, "Satellite Microwave Observations of the Utah Great Salt Lake Desert," Radio Science, Vol 10, No. 11, p 947-963, November 1975.
6. "Skylab Program Sensor Performance Report," MSC-05528, Vol VI (S194), September 1974.
7. R. H. Pflieger, "Spaceborne Hybrid MIC PIN Diode Radiometer Switch," IEEE GMTT International Symposium, 1973.
8. D. H. Hornbostel, "Hot and Cold Body Reference Noise Generators From 0 to 40 GHz," IEEE Trans. on Instrumentation and Measurement, Vol IM-23, No. 2, p 120-131, June 1974.
9. S. Becker, "Self-Balancing Radiometer," NASA SP-5972 (03), p 4-5, May 1975.
10. T. Schmugge, P. Gloersen, T. Wilhert, and F. Geiger, "Remote Sensing of Soil Moisture With Microwave Radiometers," Journal of Geophysical Research, Vol 79, No. 2, p 317-323, 10 January 1974.
11. A. Basharinov, L. Bowdin, and A. Shutko, "Passive Microwave Sensing of Moist Soils," Proc of Ninth International Symposium on Remote Sensing of Environment, Vol I, p 363-367, 19 April 1974.
12. R. Newton, S. Lee, and J. Rouse, "On The Feasibility of Remote Monitoring of Soil Moisture With Microwave Sensors," Proc of Ninth International Symposium on Remote Sensing of Environment, Vol I, p 725-738, 19 April 1974.

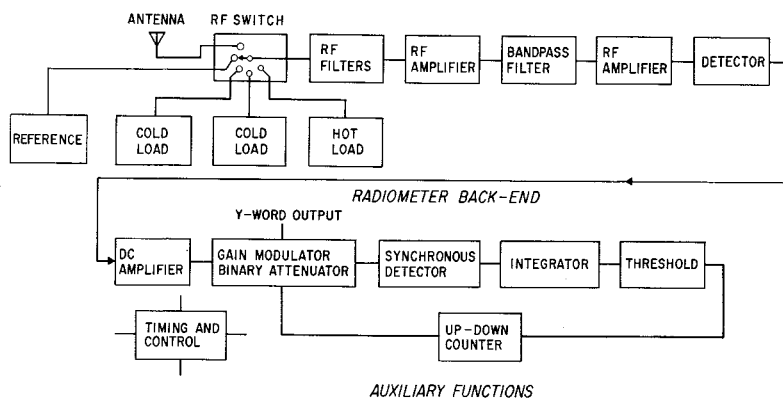


Fig. 1. Simplified Block Diagram of L-Band Radiometer

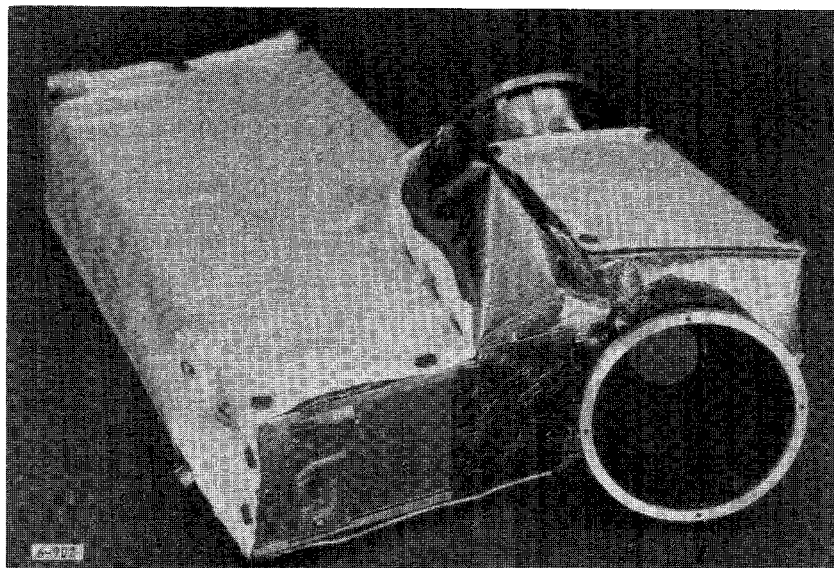


Fig. 2. Radiometer Electronics

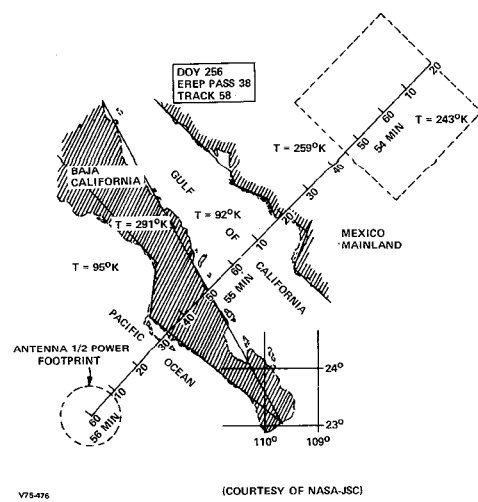


Fig. 3. S-194 Ground Track Over Baja California with Assumed Surface Brightness Temperatures

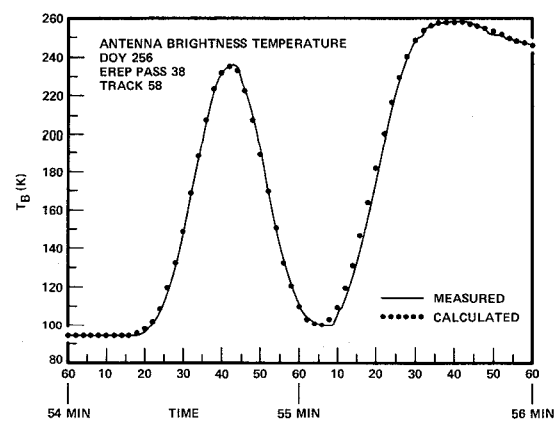


Fig. 4. Predicted and Measured Brightness Over Baja California